

Maximum Entropy Differential Dynamic Programming

Oswin So, Ziyi Wang and Evangelos A. Theodorou

Abstract—In this paper, we present a novel maximum entropy formulation of the Differential Dynamic Programming algorithm and derive two variants using unimodal and multimodal value functions parameterizations. By combining the maximum entropy Bellman equations with a particular approximation of the cost function, we are able to obtain a new formulation of Differential Dynamic Programming which is able to escape from local minima via exploration with a multimodal policy. To demonstrate the efficacy of the proposed algorithm, we provide experimental results using four systems on tasks that are represented by cost functions with multiple local minima and compare them against vanilla Differential Dynamic Programming. Furthermore, we discuss connections with previous work on the linearly solvable stochastic control framework and its extensions in relation to compositionality.

I. INTRODUCTION

Existing methods for trajectory-optimization solve the optimization problem by iteratively relying on local information via derivatives [1, 2]. Differential Dynamic Programming (DDP) [3] is a popular trajectory optimization method for nonlinear systems used in model-based Reinforcement Learning (RL) and Optimal Control problems, where the problem is iteratively solved via second order approximations of the cost and dynamics. With stage-wise positive Hessian matrices, DDP enjoys quadratic convergence [4]. However, these methods usually only guarantee convergence to a local minimum and are unable to reach better local minima once converged. In cases where there are dynamic obstacles, the cost landscape can be highly nonconvex with suboptimal local minima that are unsatisfactory. As such, there have been a handful of methods over the years which try to address this problem of local minima through techniques such as random restarts [5] or via more topological approaches which explicitly consider the different trajectory homotopies [6, 7].

Maximum entropy is a technique widely used in RL and Stochastic Optimal Control (SOC) to improve the robustness of stochastic policies. Performance robustness is achieved through an additional entropy regularization term in the cost function that improves exploration [8, 9]. In RL, Soft Actor Critic uses a maximum entropy objective and is considered to be state of the art for off-policy methods [10]. In SOC, the Information Theoretic Model Predictive Path Integral (IT-MPPI) algorithm [11, 12] is a generalization of this technique which uses the forward Kullback-Leibler (KL) divergence between the controlled distribution and a prior distribution for regularization. The form of maximum entropy is recovered when the uniform distribution is used as the prior

distribution. In [13, 14], the Tsallis divergence, a generalization of the KL divergence, is used as a regularization term in the objective, leading to further robustness improvements.

In this paper, we consider discrete time deterministic optimal control problems and take a *relaxed control* approach with entropy regularization similar to [15]. We propose two novel variations of DDP under the Maximum Entropy Optimal Control (MEOC) formulation using unimodal and multimodal Gaussian policies. In addition, we discuss the connection of our work to optimal control compositionality law [16]. Finally, we compare the performance of both proposed algorithms against vanilla DDP on 2D Point Mass, 2D Car, Quadcopter and Manipulator in simulation.

The main contributions of this work are threefold:

- We derive the Bellman equation for the discrete time MEOC problem.
- We propose the algorithms Maximum Entropy DDP (ME-DDP) and Multimodal Maximum Entropy DDP (MME-DDP) to improve exploration over vanilla DDP.
- We showcase the benefit of the improved exploration of ME-DDP and MME-DDP over vanilla DDP in converging to better local minima on four different systems in simulation.

The paper is organized as follows: In section II, we formulate the MEOC problem and derive the Bellman equation. The ME-DDP and MME-DDP algorithms are derived in sections III and IV. The connection to compositionality theory is discussed in section V, and a description of the proposed algorithms can be found in section VI. Finally, we show simulation results and conclude the paper in sections VII and VIII.

II. MAXIMUM ENTROPY BELLMAN EQUATION

Standard discrete-time deterministic optimal control problems minimize the cost over time horizon $(0, 1, \dots, T)$

$$J(u) = \Phi(x_T) + \sum_{t=0}^{T-1} l_t(x_t, u_t), \quad (1)$$

where l_t and Φ are the running and terminal costs respectively. The state and control trajectories, $(x_t)_{t=0, \dots, T}, x_t \in \mathbb{R}^{n_x}$ and $(u_t)_{t=0, \dots, T-1}, u_t \in \mathbb{R}^{n_u}$, satisfy deterministic dynamics

$$x_{t+1} = f(x_t, u_t). \quad (2)$$

In this work, we take a *relaxed control* approach and consider a stochastic control policy $\pi_t(u_t|x_t)$ with the same deterministic dynamics as in (2). In addition, we introduce

an entropy term to the original objective (1)

$$J(\pi) = \mathbb{E} \left[\Phi(x_T) + \sum_{t=0}^{T-1} \left(l_t(x_t, u_t) - \frac{1}{\alpha} H[\pi_t(\cdot|x_t)] \right) \right],$$

where $\alpha > 0$ is an inverse temperature term, the expectation is taken with respect to $u \sim \pi(\cdot|x)$, and $H[\pi]$ is the Shannon entropy of π defined as

$$H[\pi] = -\mathbb{E}[\log \pi] = -\int \pi(u) \log \pi(u) du.$$

For this problem formulation and the standard value function definition of $V(x) = \min_{\pi} J(x, \pi)$, the Bellman equation takes the form

$$V(x) = \inf_{\pi} \left\{ \mathbb{E}[l(x, u) + V'(f(x, u))] - \frac{1}{\alpha} H[\pi(\cdot|x)] \right\}, \quad (3)$$

In (3) and below we omit the time index t for nonterminal times for simplicity and use $V'(f(x, u))$ to denote the value function at the next timestep. The optimal policy here is a Gibbs distribution [13, 15]

$$\pi(u|x) = Z(x)^{-1} \exp \left(-\frac{1}{\alpha} [V'(f(x, u)) + l(x, u)] \right), \quad (4)$$

where Z denotes the partition function

$$Z(x) = \int \exp \left(-\frac{1}{\alpha} [V'(f(x, u)) + l(x, u)] \right) du.$$

Plugging the optimal policy (4) back into the Bellman equation (3) and simplifying gives us the following equation

$$V(x) = -\alpha \ln Z(x). \quad (5)$$

As we will see later, the above equation becomes easier to work with when considering the exponential transformation of the original cost and value functions. For notational simplicity, define \mathcal{E}_{α} to be the following function:

$$\mathcal{E}_{\alpha}(y) := \exp \left(-\frac{1}{\alpha} y \right). \quad (6)$$

We now define the following terms

$$r := \mathcal{E}_{\alpha}(l), \quad r_T := \mathcal{E}_{\alpha}(\Phi), \quad z := \mathcal{E}_{\alpha}(V). \quad (7)$$

With this transformation, note that the *desirability* function z is exactly the partition function Z from (5) and is linear in both z' and r (denoting z' for the next timestep):

$$\begin{cases} z(x) = Z(x) = \int z'(f(x, u)) r(x, u) du, & (8a) \\ z_T(x_T) = r_T(x_T). & (8b) \end{cases}$$

With this transformation, the optimal policy in (4) has the following elegant form

$$\pi(u|x) = z(x)^{-1} z'(f(x, u)) r(x, u). \quad (9)$$

III. MAXIMUM ENTROPY DDP

We will now use DDP to solve the MEOC problem and derive the ME-DDP algorithm. For notational simplicity, we will drop the second-order approximation of the dynamics as in iterative Linear Quadratic Regulator (iLQR) in our description of DDP. The dropped second-order dynamics terms can easily be added back in the derivations below. We refer readers to [3, 17] for a detailed overview of the vanilla DDP and iLQR algorithms.

The DDP algorithm consists of a forward pass and a backward pass. The forward pass simulates the dynamics forward in time obtaining a set of nominal state and control trajectories $(\bar{x}_{0:T}, \bar{u}_{0:T-1})$, while the backward pass solves the Bellman equation with a 2nd order approximation of the costs and dynamics equations around the nominal trajectories. The boundary conditions for the value function V are obtained by performing a 2nd order Taylor expansion of the terminal cost Φ :

$$V_{xx,T} = \Phi_{xx}, \quad V_{x,T} = \Phi_x, \quad V_T = \Phi. \quad (10)$$

To derive the backward pass, we first perform a quadratic approximation of the cost function around (\bar{x}, \bar{u})

$$l(x, u) \approx l(\bar{x}, \bar{u}) + \begin{bmatrix} l_x \\ l_u \end{bmatrix}^T \begin{bmatrix} \delta x \\ \delta u \end{bmatrix} + \frac{1}{2} \begin{bmatrix} \delta x \\ \delta u \end{bmatrix}^T \begin{bmatrix} l_{xx} & l_{xu} \\ l_{ux} & l_{uu} \end{bmatrix} \begin{bmatrix} \delta x \\ \delta u \end{bmatrix},$$

where $\delta x := x - \bar{x}$, $\delta u := u - \bar{u}$. We also perform a linear approximation of the dynamics f :

$$f(x, u) \approx f(\bar{x}, \bar{u}) + f_x^T \delta x + f_u^T \delta u.$$

Performing a Taylor expansion of the $V'(x) + l = Q$ term in the Bellman equation (3) with respect to x and u , we obtain the following

$$\begin{aligned} V'(x) + l &\approx V'(f(\bar{x}, \bar{u})) + l(\bar{x}, \bar{u}) + \delta Q, \\ \delta Q &:= \begin{bmatrix} Q_x \\ Q_u \end{bmatrix}^T \begin{bmatrix} \delta x \\ \delta u \end{bmatrix} + \frac{1}{2} \begin{bmatrix} \delta x \\ \delta u \end{bmatrix}^T \begin{bmatrix} Q_{xx} & Q_{xu} \\ Q_{ux} & Q_{uu} \end{bmatrix} \begin{bmatrix} \delta x \\ \delta u \end{bmatrix}. \end{aligned}$$

By completing the square and plugging the above into the form of the optimal policy (4), we obtain the optimal policy

$$\pi^*(\delta u|\delta x) \propto \exp \left(-\frac{1}{\alpha} \left[\frac{1}{2} (\delta u - \delta u^*)^T Q_{uu} (\delta u - \delta u^*) \right] \right), \quad (11)$$

where the optimal deviation from the nominal controls δu^* has the same form as the vanilla DDP case

$$\delta u^* = -Q_{uu}^{-1} (Q_{ux} \delta x + Q_u) = K \delta x + k. \quad (12)$$

We see that the optimal policy (11) is a multivariate Gaussian distribution with mean $\bar{x} + \delta u^*$ and covariance αQ_{uu}^{-1} . Plugging this into the Taylor expansion of the Bellman equation (3), we see that

$$V(\bar{x} + \delta x) = \bar{V}(x) + V_H(\bar{x}) + V_x(\bar{x})^T \delta x + \frac{1}{2} \delta x^T V_{xx}(\bar{x}) \delta x,$$

where the terms \bar{V} , V_H , V_x and V_{xx} have the form

$$\bar{V}(\bar{x}) = \bar{V}'(\bar{x}) + l(\bar{x}, \bar{u}) - \frac{1}{2} Q_u^T Q_{uu} Q_u, \quad (13)$$

$$V_H(\bar{x}) = \frac{\alpha}{2} \ln \left(|Q_{uu}| - n_u \ln(2\pi\alpha) \right), \quad (14)$$

$$V_x(\bar{x}) = Q_x + K^T Q_{uu} k + K^T Q_u + Q_{ux}^T k, \quad (15)$$

$$V_{xx}(\bar{x}) = Q_{xx} + K^T Q_{uu} K + K^T Q_{ux} + Q_{ux}^T K. \quad (16)$$

Note that the update rules for \bar{V} , V_x and V_{xx} are exactly the same as in vanilla DDP, with the only difference being the addition of the V_H term, which results from the Shannon entropy of a Gaussian distribution and approaches 0 as $\alpha \rightarrow 0$.

IV. MULTIMODAL MAXIMUM ENTROPY DDP

While a unimodal Gaussian policy is able to achieve better exploration compared to the deterministic policy, it is often the case that multiple modes need to be explored simultaneously to converge to the global minimum [9]. In this section, we derive a multimodal extension to the ME-DDP introduced.

Let $\{\bar{x}^{(n)}, \bar{u}^{(n)}\}_{n=1}^N$ be N different nominal state and control trajectories, and let $\Phi^{(n)}$ corresponds to the respective quadratic approximation of Φ around $\bar{x}^{(n)}$ and $\bar{u}^{(n)}$. Instead of using a single quadratic approximation of Φ for the terminal cost as in (10), we use the combined approximation $\tilde{\Phi}$

$$V_T(x_T) = \tilde{\Phi}(x_T) := -\alpha \ln \sum_{n=1}^N \exp \left(-\frac{1}{\alpha} \Phi^{(n)}(x_T) \right). \quad (17)$$

The log-sum-exp is a smoothed combination of the local quadratic approximation and approaches $\min_n \{\Phi^{(n)}\}$ as α approaches 0, as shown in Fig. 1. Writing (17) using the desirability function z we obtain a much cleaner form

$$z_T(x_T) = \sum_{n=1}^N z_T^{(n)}(x_T), \quad z_T^{(n)}(x_T) := r^{(n)}(x_T).$$

Suppose that $z'(x) = \sum_{n=1}^N z'^{(n)}(x)$. Substituting this in (8a) for z , we get

$$\begin{aligned} z(x) &= \int \left(\sum_{n=1}^N z'^{(n)}(f(x, u)) \right) r(x, u) du, \\ &= \sum_{n=1}^N \int z'^{(n)}(f(x, u)) r(x, u) du, \\ &= \sum_{n=1}^N z^{(n)}(x). \end{aligned} \quad (18)$$

By induction, the additive structure of the Bellman equation is preserved when taking the following update rule for $z^{(n)}$

$$z^{(n)}(x) = \int z'^{(n)}(f(x, u)) r(x, u) du, \quad (19)$$

which is identical to (8a). In other words, each $z^{(n)}$ and $V^{(n)}$ is computed in exactly the same way as z and V in the unimodal case but uses a different terminal condition $\Phi^{(n)}$. Additionally, substituting V back for z in (18) yields

$$V(x) = -\alpha \ln \sum_{n=1}^N \exp \left(-\frac{1}{\alpha} V^{(n)}(x) \right). \quad (20)$$



Fig. 1: Comparison of the individual quadratic approximation (top) and the log-sum-exp approximation (bottom) of the cost function $l(x)$ with varying choices of inverse temperature α . Higher α leads to smoother approximation.

This result makes sense intuitively—the combined value function should be related to the minimum of the individual approximated value functions resulting from the different nominal states.

Using the linearity of the desirability function (18), the optimal policy (9) has the form

$$\begin{aligned} \pi(u|x) &= z(x)^{-1} \left(\sum_{n=1}^N z'^{(n)}(f(x, u)) \right) r(x, u), \\ &\propto \sum_{n=1}^N \frac{z^{(n)}(x)}{z(x)} z'^{(n)}(f(x, u)) r(x, u), \\ &= \sum_{n=1}^N w^{(n)}(x) \pi^{(n)}(u|x), \end{aligned} \quad (21)$$

where

$$\begin{aligned} \pi^{(n)}(u|x) &:= z^{(n)}(x)^{-1} z'^{(n)}(f(x, u)) r(x, u), \\ w^{(n)}(x) &:= z(x)^{-1} z^{(n)}(x), \quad \sum_{n=1}^N w^{(n)} = 1. \end{aligned}$$

This is exactly the policy obtained in the normal case, except that we consider $z^{(n)}$ instead of z . Since $V^{(n)}$ is quadratic in the state, each $\pi^{(n)}$ will be Gaussian as before:

$$\begin{aligned} \pi^{(n)}(\delta u^{(n)} | \delta x^{(n)}) &\propto \exp \left(-\frac{1}{\alpha} \left[\frac{1}{2} (\delta u^{(n)} - \delta u^{(n)*})^T Q_{uu}^{(n)} (\delta u^{(n)} - \delta u^{(n)*}) \right] \right), \end{aligned} \quad (22)$$

where $\delta x^{(n)} = x - \bar{x}^{(n)}$ and $\delta u^{(n)} = u - \bar{u}^{(n)}$ are now evaluated relative to the nominal trajectories for corresponding to the n th approximation, with $\delta u^{(n)*}$ defined analogous to (12) but using the approximations around $(\bar{x}^{(n)}, \bar{u}^{(n)})$. Importantly, from the form of (21), we see that π is a mixture of Gaussians with component weights $w^{(n)}$.

Since both z and π are weighted sums of $z^{(n)}$ and $\pi^{(n)}$, computing the solution to the backward pass of MME-DDP is equivalent to solving for ME-DDP around the N different nominal trajectories and then *composing* the value functions and policies using (20) and (21).

Algorithm 1: Backward Pass

```
1 Compute  $V(T), V_x(T)$  and  $V_{xx}(T)$  using  $\Phi$ 
2 for  $t = T - 1$  to 0 do
3   Compute  $l, Q$  and their derivatives for timesteps  $t$ 
4   Regularize  $Q_{uu}$  to be PD
5   Compute  $k_t, K_t, V_x(t-1), V_{xx}(t-1)$  as in
     Vanilla DDP
6    $\Sigma_t \leftarrow \alpha Q_{uu}^{-1}$ 
7    $V_H \leftarrow V_H + \frac{\alpha}{2}(\ln|Q_{uu}| - n_u \ln(2\pi\alpha))$ 
```

Algorithm 2: (Unimodal) Maximum Entropy DDP

Input: Number of iterations K , Resample frequency m

```
1 Initialize  $x^{(1:2)}, u^{(1:2)}, K^{(1:2)}, \Sigma^{(1:2)}, \pi$ 
2 for  $k = 1$  to  $K$  do
3   if  $k \% m = 0$  then
4     Set  $x^{(1)}, u^{(1)}, K^{(1)}, \Sigma^{(1)}$  to the mode with the
       lowest cost and update  $\pi$  with it.
5     Sample  $x^{(2)}, u^{(2)}, K^{(2)}$  from  $\pi$ 
6   for  $n = 1$  to 2 in parallel do
7      $x^{(n)} \leftarrow$  Rollout dynamics
8      $k^{(n)}, K^{(n)}, \Sigma^{(n)}, V_H^{(n)} \leftarrow$  Backward Pass
9      $x^{(n)}, u^{(n)}, J^{(n)} \leftarrow$  Line Search
```

V. CONNECTIONS TO COMPOSITIONALITY AND LINEAR SOLVABLE OPTIMAL CONTROL

A key component of our work is the compositionality of policies—solving for the full policy π by first solving for the individual policies $\pi^{(n)}$, then combining them via (21). However, this topic is not new in the field. In [16], the KL Divergence regularized control is considered and the compositionality of controllers is introduced by exploiting the linearity of the exponential value function and the optimal policy. The KL Divergence is only used as a control cost in [16], whereas our work is more general and allows for the running cost $l(x, u)$ to be an arbitrary function of the controls u . Additionally, unlike their work, we provide practical algorithms using this compositionality principle in the form of ME-DDP and MME-DDP. Similarly, in the field of RL [18], compositionality law has been used on maximum entropy optimal policies to solve a conjunction of tasks by combining maximum entropy policies which solve each of the tasks individually.

Unlike the above works, the approach our work takes focuses on the topic of exploration rather than compositionality. Our work is most similar to [9], which shows that the multimodal exploration achieved via a neural-network parametrized value function and policy network are able to outperform similar methods which only consider unimodal exploration policies. However, unlike [9], we make use of compositionality and solve for the value function explicitly using DDP, which allows for the policy to be computed online in realtime without prior pretraining.

Algorithm 3: Multimodal Maximum Entropy DDP

Input: Number of GMM components N , Number of iterations K , Resample frequency m

```
1 Initialize  $x^{(1:N)}, u^{(1:N)}, K^{(1:N)}, \Sigma^{(1:N)}, \pi$ 
2 for  $k = 1$  to  $K$  do
3   if  $k \% m = 0$  then
4     Set  $x^{(1)}, u^{(1)}, K^{(1)}$  to the mode with the
       lowest cost
5     Sample  $x^{(2:N)}, u^{(2:N)}, K^{(2:N)}$  from GMM  $\pi$ 
       with weights  $w^{(1:N)}$ 
6   for  $n = 1$  to  $N$  in parallel do
7      $x^{(n)} \leftarrow$  Rollout dynamics
8      $k^{(n)}, K^{(n)}, \Sigma^{(n)}, V_H^{(n)} \leftarrow$  Backward Pass
9      $x^{(n)}, u^{(n)}, J^{(n)} \leftarrow$  Line Search
10    Compute  $w^{(n)}$  using  $J^{(n)}$  and  $V_H^{(n)}$ 
```

VI. ALGORITHMS

There are three main algorithmic issues that need to be addressed when implementing ME-DDP and MME-DDP.

Forward Pass: The derivation in earlier sections only describes how to perform the backward pass of DDP to compute the optimal Gaussian mixture policy (21), leaving the question of how to apply the new stochastic policy for the forward pass unanswered.

For the case of ME-DDP, one option is to ignore the stochasticity of the unimodal policy and simply apply the controls corresponding to the mean of the Gaussian policy for each timestep. However, this is identical to the case of vanilla DDP, defeating the point of the maximum entropy framework. Hence, we decide to perform multiple realizations of the stochastic policy at each timestep. Taking N realizations for each of the T timesteps will result in the polynomial growth $O(T^N)$ of the required number of samples. Instead, we sample the entire feedforward controls from the stochastic policy at $t = 0$ and then apply the deterministic feedback policy for times $t = 1$ to $T - 1$.

To handle the added multi-modality of the optimal MME-DDP policy, we sample from a categorical distribution to determine which of the N modes will be used for the control of a particular sample trajectory, and then sample the feedforward controls as in the ME-DDP case.

Convergence: With a stochastic policy, the cost of the trajectory after sampling may be higher in cost than the original trajectory or even unbounded. To guarantee the convergence of the algorithms, we draw inspirations from the technique of replica exchange [19] and apply the mean deterministic controls from the mode with the smallest cost to at least one sampled trajectory. This guarantees that the minimum cost over all N samples is monotonically decreasing, preserving the convergence properties of DDP.

Frequency of Sampling: Since the weights $w^{(n)}$ for each mode for MME-DDP are proportional to the value function $Z^{(n)}$, modes which have high cost are unlikely to be resampled in the next iteration of the forward pass even if will converge to a more optimal local minimum given enough

TABLE I: Comparison of the mean and standard deviations of the cost for vanilla DDP, ME-DDP and MME-DDP, computed on 16 different DDP runs. The best mean cost for each system is boldfaced. The mean reduction percentages are included to the right where positive values correspond to a reduction. Significant reduction in mean and standard deviation can be observed from MME over both ME and vanilla DDP.

System	Vanilla		ME		MME		MME vs Vanilla	MME vs ME
	Mean	Std	Mean	Std	Mean	Std	$\Delta\text{Mean}\%$	$\Delta\text{Mean}\%$
2D Point Mass	32.25	0.00	10.76	9.55	1.76	0.00	94.55	83.69
Car	5.31	0.00	4.99	0.64	3.76	0.87	29.16	24.63
Quadcopter	0.98	0.00	0.90	0.18	0.54	0.02	45.08	40.25
Manipulator	22.84	0.00	20.28	4.68	12.56	3.68	45.00	38.06

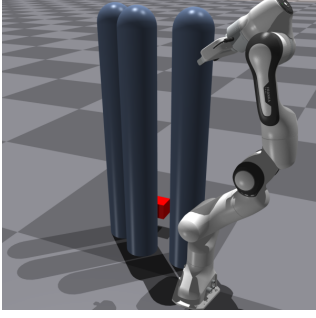


Fig. 2: Task setup for the manipulator. The goal is to reach the red block past the obstacles while avoiding collisions.

DDP iterations. To alleviate this issue, we only resample the controls for each mode after every m iterations, increasing the probability of jumping out of suboptimal local minima.

Having addressed all of the above issues, the full ME-DDP and MME-DDP algorithms are presented in Algorithm 2 and Algorithm 3, along with their backward pass in Algorithm 1, where variables without indices denote the entire trajectory, $(x^{(n)})$ denotes $x_{0:T}^{(n)}$. In short, both algorithms consist of keeping the lowest cost sample and sampling the rest from the stochastic policy π every m iterations for the forward pass, then running the backward pass for each sample. Both passes can be executed in parallel for each sample.

VII. SIMULATIONS

In this section, we compare the performance of the proposed MME-DDP algorithm against the unimodal ME-DDP and vanilla DDP algorithms on four systems: 2D Point Mass, 2D Car, Quadcopter and Manipulator. Obstacle avoidance is implemented as a soft-constraint by augmenting the state cost with $l_{\text{obs}} = \exp\left(-\frac{d_{\text{obs}}^2}{2r_{\text{obs}}^2}\right)$, where d_{obs} and r_{obs} are the distance to the obstacle and the radius of the obstacle respectively. The controls are initialized to the zero controls for all systems. For the resampling frequency, we set $m = 8$. All DDP variants are implemented in Python using JAX [20].

A. 2D Point Mass

We first test the algorithms on an illustrative 2D point-mass double integrator system. The task is for the point-mass to reach a target location while avoiding obstacles in a maze-like environment via one of three paths. Both the top and middle paths are suboptimal local minima as they are blocked by obstacles, with the top path having an obstacle near the end of the path. The results are shown in the first row of Fig. 3.

B. 2D Car

We next test on a 2D Car with dynamics of Dubin's vehicle under jerk control. The system has state $x = [p_x, p_y, \theta, v, a]^T \in \mathbb{R}^5$ and controls $u = [\omega, j]^T \in \mathbb{R}^2$, where (p_x, p_y) describe the car's position, v, a, j are the linear velocity, acceleration and jerk, and θ, ω are the orientation and angular velocity. The task here is again a reaching task while avoiding two circular obstacles. A suboptimal local minimum exists in the middle which goes in between both obstacles. The results are shown in the second row of Fig. 3.

C. Quadcopter

We test on a 3D quadcopter with states $x = [p_x, p_y, p_z, \Psi, \theta, \phi, v_x, v_y, v_z, p, q, r]^T \in \mathbb{R}^{12}$ and controls $u = [f_t, \tau_x, \tau_y, \tau_z]^T \in \mathbb{R}^4$. We refer readers to [21] for a full description of the dynamics.

The task is to reach a target on the other side of four spherical obstacles set up in a square pattern. A suboptimal local minima is present in the intersection of all four obstacles in the center which only MME-DDP is able to consistently escape from, as shown in the third row of Fig. 3.

D. Manipulator

Finally, we test on a torque-controlled 7-DOF manipulator based off a simplified version of the Franka EMIKA Panda arm with states $x = [\theta_0, \dots, \theta_6, \dot{\theta}_0, \dots, \dot{\theta}_6]^T \in \mathbb{R}^{14}$ and controls $u = [\tau_0, \dots, \tau_6]^T \in \mathbb{R}^7$, where $(\theta_{2i}, \theta_{2i+1}), i = 0, \dots, 3$ corresponds to the pitch and yaw angles for each of the 4 joints (only yaw for the last joint), $\dot{\theta}_i$ denotes the angular velocity, and τ_i denotes the torque control.

The task here is for the end effector to reach the goal position without colliding with obstacles (see Fig. 2). Cylindrical obstacles are placed between the starting position and the end effector, creating multiple suboptimal local minima in the cost landscape. Again, only MME-DDP is able to consistently reach the target without intersecting any of the obstacles, as shown in the bottom row of Fig. 3.

Performance Comparison: Comparing the trajectories between the three algorithms across the 4 systems, we observe that in the case of one global minimum and several local minima (Point Mass and Manipulator), vanilla DDP gets stuck in a local minimum. Unimodal ME-DDP explores several minima but lacks the representational capability to explore each sufficiently. In contrast, the additional exploration capability helps MME-DDP find the best minimum. In the case of many minima of similar cost (Car and Quadcopter), vanilla and

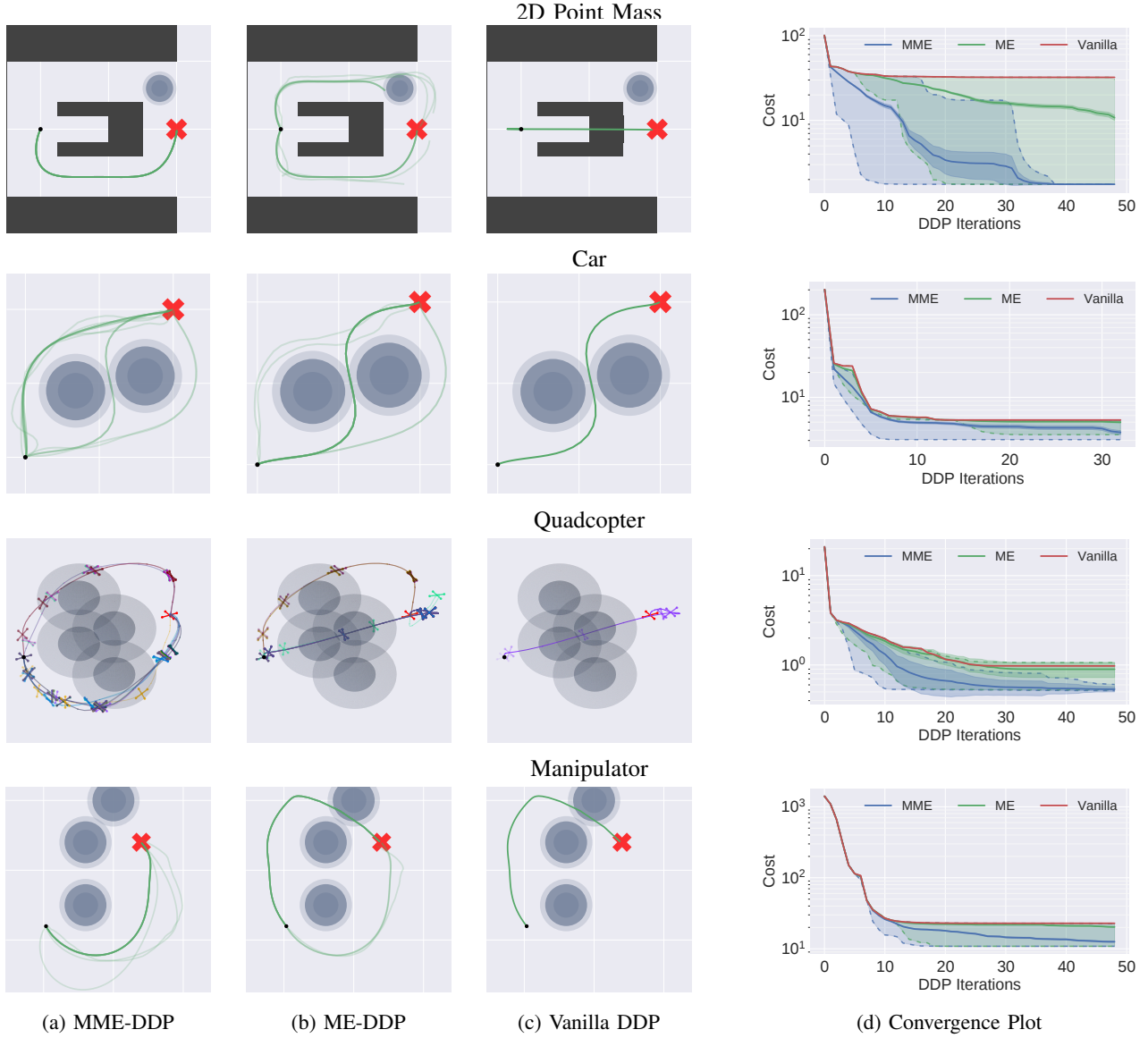


Fig. 3: (a)–(c) Position trajectories for the 2D point mass, car, quadcopter and manipulator systems from 16 different DDP runs. The black and red markers represent the initial and target positions respectively for each task. For the quadcopter, each color represents the trajectories from a single DDP run. For the manipulator, the projections of the end effector trajectories on the XY-plane are plotted. (d) Convergence plots for all three algorithms. The solid line denotes the mean, the dark shaded region represents the 2σ relative uncertainty, while the dotted lines denote the minimum and maximum costs. In all examples, MME-DDP is able to converge to a better global minimum due to having better exploration.

ME-DDP mostly get stuck in one or few suboptimal minima while MME-DDP explores several minima simultaneously. Note that as the obstacles are implemented as a soft constraint, the shaded region around obstacles in Fig. 3 only provides a visualization for the obstacle cost and **not** the obstacle boundary. We also present a comparison of convergence for each algorithm in Table I and Fig. 3d. Across all tasks, it is clear that both ME-DDP and MME-DDP are able to achieve a lower mean cost than vanilla DDP due to converging to a more optimal local minimum as a result of the improved exploration capabilities. Furthermore, MME-DDP is able to consistently achieve a significantly lower cost, highlighting the advantages of multimodal exploration.

VIII. CONCLUSION

In this paper, we derived ME-DDP and MME-DDP, two algorithms based off the maximum entropy formulation of DDP which provide improved exploration capabilities over the vanilla algorithm. Our results suggest that the added stochasticity and multimodal exploration improves the ability of DDP to escape from suboptimal local minima in environments with multiple local minima.

Future work include hardware implementation to verify the exploration benefits of the proposed algorithms. On the theoretical side we will investigate the conditions and rate of convergence, as well as generalizations that include the stochastic, risk sensitive and model predictive control cases.

REFERENCES

- [1] Lev Semenovich Pontryagin. Mathematical theory of optimal processes. CRC press, 1987.
- [2] Mustafa Mukadam, Xinyan Yan, and Byron Boots. Gaussian process motion planning. In 2016 IEEE international conference on robotics and automation (ICRA), pages 9–15. IEEE, 2016.
- [3] David Mayne. A second-order gradient method for determining optimal trajectories of non-linear discrete-time systems. International Journal of Control, 3(1): 85–95, 1966.
- [4] L-Z Liao and Christine A Shoemaker. Convergence in unconstrained discrete-time differential dynamic programming. IEEE Transactions on Automatic Control, 36(6):692–706, 1991.
- [5] Helen Oleynikova, Michael Burri, Zachary Taylor, Juan Nieto, Roland Siegwart, and Enric Galceran. Continuous-time trajectory optimization for online uav replanning. In 2016 IEEE/RSJ international conference on intelligent robots and systems (IROS), pages 5332–5339. IEEE, 2016.
- [6] Christoph Rösmann, Frank Hoffmann, and Torsten Bertram. Integrated online trajectory planning and optimization in distinctive topologies. Robotics and Autonomous Systems, 88:142–153, 2017.
- [7] Boyu Zhou, Fei Gao, Jie Pan, and Shaojie Shen. Robust real-time uav replanning using guided gradient-based optimization and topological paths. In 2020 IEEE International Conference on Robotics and Automation (ICRA), pages 1208–1214. IEEE, 2020.
- [8] Brian D Ziebart. Modeling purposeful adaptive behavior with the principle of maximum causal entropy. PhD thesis, Carnegie Mellon University, 2010.
- [9] Tuomas Haarnoja, Haoran Tang, Pieter Abbeel, and Sergey Levine. Reinforcement learning with deep energy-based policies. In International Conference on Machine Learning, pages 1352–1361. PMLR, 2017.
- [10] Tuomas Haarnoja, Aurick Zhou, Pieter Abbeel, and Sergey Levine. Soft actor-critic: Off-policy maximum entropy deep reinforcement learning with a stochastic actor. In International conference on machine learning, pages 1861–1870. PMLR, 2018.
- [11] Grady Williams, Nolan Wagener, Brian Goldfain, Paul Drews, James M Rehg, Byron Boots, and Evangelos A Theodorou. Information theoretic mpc for model-based reinforcement learning. In 2017 IEEE International Conference on Robotics and Automation (ICRA), pages 1714–1721. IEEE, 2017.
- [12] Ziyi Wang, Grady Williams, and Evangelos A Theodorou. Information theoretic model predictive control on jump diffusion processes. In 2019 American Control Conference (ACC), pages 1663–1670. IEEE, 2019.
- [13] Ziyi Wang, Oswin So, Jason Gibson, Bogdan Vlahov, Manan Gandhi, Guan-Horng Liu, and Evangelos Theodorou. Variational Inference MPC using Tsallis Divergence. In Proceedings of Robotics: Science and Systems, Virtual, July 2021. doi: 10.15607/RSS.2021.XVII.073.
- [14] Kyungjae Lee, Sungyub Kim, Sungbin Lim, Sungjoon Choi, Mineui Hong, Jaemin Kim, Yong-Lae Park, and Songhwai Oh. Generalized tsallis entropy reinforcement learning and its application to soft mobile robots. Robotics: Science and Systems Foundation, 2020.
- [15] Jeongho Kim and Insoon Yang. Hamilton-jacobi-bellman equations for maximum entropy optimal control. arXiv preprint arXiv:2009.13097, 2020.
- [16] Emanuel Todorov. Compositionality of optimal control laws. Advances in neural information processing systems, 22:1856–1864, 2009.
- [17] Weiwei Li and Emanuel Todorov. Iterative linear quadratic regulator design for nonlinear biological movement systems. In ICINCO (1), pages 222–229. Citeseer, 2004.
- [18] Tuomas Haarnoja, Vitchyr H. Pong, Aurick Zhou, Murata Dalal, P. Abbeel, and Sergey Levine. Composable deep reinforcement learning for robotic manipulation. 2018 IEEE International Conference on Robotics and Automation (ICRA), pages 6244–6251, 2018.
- [19] Jing Dong and Xin T Tong. Replica exchange for non-convex optimization. Journal of Machine Learning Research, 22(173):1–59, 2021.
- [20] James Bradbury, Roy Frostig, Peter Hawkins, Matthew James Johnson, Chris Leary, Dougal Maclaurin, George Nectra, Adam Paszke, Jake VanderPlas, Skye Wanderman-Milne, and Qiao Zhang. JAX: composable transformations of Python+NumPy programs, 2018. URL <http://github.com/google/jax>.
- [21] Francesco Sabatino. Quadrotor control: modeling, nonlinear control design, and simulation. Master’s thesis, KTH Royal Institute of Technology, 2015.